Progress in Nuclear Energy 86 (2016) 11–17

Contents lists available at ScienceDirect

Progress in Nuclear Energy

journal homepage: www.elsevier.com/locate/pnucene

^{236}U resonance parameters at 5.467 eV from neutron transmission measurements using thin liquid samples

D.P. Barry [a, *], M.J. Rapp [a], R.C. Block [a], B.E. Epping [a], G. Leinweber [a], Y. Danon [b], A. Daskalakis [b], E. Blain [b], B. McDermott [b]

[a] Bechtel Marine Propulsion Corp., Knolls Atomic Power Laboratory, P.O. Box 1072, Schenectady, NY 12301, United States
[b] Rensselaer Polytechnic Institute, Gaerttner LINAC Center, 110 8th St., Troy, NY 12180, United States

ARTICLE INFO

Article history:
Received 1 May 2015
Received in revised form 30 September 2015
Accepted 1 October 2015
Available online xxx

Keywords:
Resonance parameters
Transmission
Uranium-236
Total cross section
RPI

ABSTRACT

The ^{236}U isotope is an important buildup product that is generated in the ^{235}U fuel cycle and influences reactor neutronic calculations. The aim of the present work is to improve upon the existing neutron total cross section data for the strong ^{236}U resonance at 5.467 eV.

High accuracy neutron transmission measurements were performed using the time-of-flight technique at the Rensselaer Polytechnic Institute linear accelerator. An approach was used to fabricate thin ^{236}U samples using liquid, allowing for non-saturated resonances. The transmission measurements were made at the 15 m flight station with a ^{6}Li glass scintillation detector. Methods to characterize the background and experimental resolution function were developed. The ^{236}U resonance parameters and their uncertainties at 5.467 eV were determined by fitting the transmission data using a Monte Carlo approach with the SAMMY multi-level R-matrix Bayesian code.

The resonance parameters determined in this work are: energy, E, equal to 5.467 ± 0.005 eV; neutron width, Γ_n, equal to 2.13 ± 0.04 meV; and radiation width, Γ_γ, equal to 27 ± 1 meV. The fission width, Γ_f, was not fitted and was fixed to the ENDF-7.1 value of 0.290 meV. These parameters gave a neutron capture resonance integral of 330 ± 5 b that is lower than all of the selected evaluations: Mughabghab by 4.7%, ENDF-7.1 by 3.7%, JEFF-3.1 by 4.8%, and JENDL-4.0 by 7.2%.

1. Introduction

^{236}U is a significant buildup product that is produced from neutron capture in the ^{235}U fuel used in a majority of nuclear power reactors. When a ^{235}U nucleus absorbs a neutron, it forms the $^{236}U^*$ compound nucleus. This compound nucleus may undergo a fission reaction or, alternatively, may decay to a ^{236}U nucleus through the capture (n,γ) reaction. The ^{235}U capture-to-fission cross section ratio at thermal energy (0.0253 eV) is approximately 17 captures per 100 fissions, or a 17% yield of ^{236}U. This is greater than the yield given for the most prevalent fission products (Baum et al., 2010). The buildup of ^{236}U influences the neutron population in a reactor core and fuel. Therefore, knowledge of the ^{236}U cross section is important to nuclear reactor design and criticality safety.

Despite its importance, very few total cross section measurements exist for the ^{236}U resonance at 5.467 eV. The extremely large peak cross section of this resonance (>13,000 b) results in zero transmission through thick samples. A transmission resonance that goes to zero is called "saturated" and much information about the peak total cross section is lost. Thin samples are difficult to fabricate to the tight tolerances needed for precision measurements. It is difficult to fabricate thin oxide powder samples as they may suffer from voids due to uneven settling and/or clumping. Other types of measurement, such as capture, self-indication, and activation have employed thin ^{236}U metal. Such thin metal samples are hard to manufacture with a uniform thickness. An approach is required which enables the use of an extremely thin ^{236}U sample to prevent the transmission from becoming saturated. Historically, such samples were fabricated using U_3O_8 oxide powder. The ^{236}U transmission measurements presented in this paper were done with the use of homogeneous liquid samples. Liquid samples have the benefit of being uniform and are much less susceptible to voids. Neutron capture measurements were not performed because they would not provide any appreciable information for this predominately capture resonance (Barry, 2003).

* Corresponding author.
E-mail address: barryd3@rpi.edu (D.P. Barry).

http://dx.doi.org/10.1016/j.pnucene.2015.10.001

A literature review was performed to find published values for the ^{236}U 5.467 eV resonance parameters using the Computer Index of Nuclear Reaction Data (CINDA, 2014). The CINDA results show the scarcity of total cross section (i.e., transmission) data for the ^{236}U resonance at 5.467 eV. Only the work of McCallum (1958) and Harvey and Hughes (1958) published resonance parameters (Table 6) resulting directly from a transmission current nuclear data evaluations because both experiments were performed prior to 1960 with poor energy resolution fast choppers and oxide powder samples. Due to the poor energy resolution, area analysis techniques were used to extract resonance parameters from the data. These experimental conditions and area analysis methods are suboptimal by modern standards. In contrast, the measurements presented in this paper have better energy resolution and do not use oxide powder samples. In addition, modern resonance shape fitting analysis techniques are used to extract the resonance parameters.

Other results from CINDA reporting ^{236}U 5.467 eV resonance parameters (Table 6) include neutron capture and self-indication measurements by Carlson et al. (1970) and the activation measurements of Baumann et al. (1968).

The ^{236}U 5.467 eV resonance parameters found in the ENDF-7.1 (Chadwick et al., 2011), JENDL-4.0 (Shibata et al., 2011), and JEFF-3.2 (Koning et al., 2006) nuclear data evaluations (Table 6) rely heavily on the evaluation of Mughabghab (1984). Because of the deficiency in ^{236}U total cross section measurements at 5.467 eV, the resonance parameters of Mughabghab are highly influenced by the work of Carlson et al. It should be noted that the evaluations do not incorporate the most recent values given by Mughabghab (2006).

Due to the lack of available total cross section data for the ^{236}U resonance at 5.467 eV and the importance of this isotope in the ^{235}U fuel cycle, we performed a new measurement at the linear accelerator (LINAC) located at Rensselaer Polytechnic Institute (RPI). This paper uses an approach to fabricate thin ^{236}U samples using liquids, allowing us to accurately determine the transmission through the 5.467 eV resonance for the first time since 1958.

2. Material and methods

As incident neutrons pass through a uniform thickness of material they may be transmitted through the sample and be detected or may undergo an interaction with the sample, such as elastic scattering or capture, preventing it from being detected. By measuring the ratio of counting rates in the detector with and without the sample in the beam the transmission can be calculated.

The transmission is related to the total cross section by the following equation:

$$T(E) = e^{-n\sigma_t(E)} \quad (1)$$

where n is the number density of the target material (units of atoms/barn) and $\sigma_t(E)$ is the total cross section at energy E in units of barns (10^{-24} cm^2).

A measurement of the ^{236}U resonance at 5.467 eV presents a significant challenge since this resonance has a very large peak cross section that can easily cause the transmission to be zero if the sample thickness (i.e., number density) is too large, rendering Equation (1) unusable when solving for the total cross section.

2.1. Liquid samples

For convenience in discussion and comparison, the experiment and results are described as “RPI-2014”. The RPI-2014 transmission experiment used three liquid samples containing different concentrations (i.e., thickness) of ^{236}U. The thickness for each sample was chosen to produce a non-saturated transmission resonance at 5.467 eV. The thickest sample provided a minimum transmission of approximately 0.1. The liquid samples were prepared by Oak Ridge National Laboratory (ORNL, 2013) by dissolving U_3O_8 oxide powder (89% enriched in ^{236}U) into deuterated nitric acid (DNO_3) to form a nitrate solution. The DNO_3 was chosen due to its low and flat neutron total cross section in the energy region of interest. The nitrate solution was then diluted with heavy water (D_2O) until the desired concentration of ^{236}U was achieved for each sample.

Each liquid sample was contained inside of a spectroscopic quartz cell (Starna, 2014). Quartz was chosen over Pyrex or glass as it contains no boron. Additionally, quartz is inert to most chemicals. The cell characteristics are shown in Table 1. The cells were slightly modified by replacing the original Teflon stoppers with glass stoppers to prevent leakage. Additionally, the stem was covered with paraffin wax to seal the glass stopper in place, thus reducing the chance for leakage. Finally, a rubber finger cut was placed over the paraffin and stem as a tertiary seal.

A 10 mm length of D_2O has a neutron transmission of approximately 0.67 that does not excessively attenuate the incident neutron beam. The diameter of the quartz cell was a third larger than the diameter of collimated neutron beam, eliminating any concern for the neutron beam impinging upon the inner diameter walls of the cell.

Mass spectrometry was performed at ORNL to determine the sample compositions. The atom percent of each isotope is shown in Table 2. The ^{236}U concentration was quoted with a 1% uncertainty in the mass spectroscopy analysis.

The number density for each isotope in the liquid samples is presented for the thick (Table 3), medium (Table 4), and thin (Table 5) liquid samples.

2.2. Experimental setup

The RPI LINAC produces a high energy pulsed neutron source (up to 60 MeV) by accelerating electrons and colliding them with a tantalum neutron production target, generating bremsstrahlung radiation and photoneutrons. The time-of-flight (TOF) technique was used to measure the neutron counting rate as a function of neutron flight time.

The neutron producing target used in this experiment is known as the Enhanced Thermal Target (ETT) (Danon, 1990). This target was selected to optimize the number of neutrons interacting in the ^{236}U resonance at 5.467 eV, thereby reducing the run time required to minimize statistical uncertainty on the collected data and improve the signal-to-background ratio.

Evacuated drift tubes were employed for a majority of the neutron flight path to the detector in order to reduce air scattering. The neutron beam was collimated to a 3.49 cm (1.375 inch) diameter beam at the sample location.

The neutron transmission experiment was performed at the 15 m flight station. The neutron detector is a 7.62 cm (3 in.) diameter, 0.3 cm thick NE-905 loaded scintillator glass (6.6% lithium, enriched in ^{6}Li to 95%) and optically coupled to a photomultiplier tube. This detector was placed directly in the beam 14.973 ± 0.005 m from the neutron production target. This detector was housed inside of a 10.16 cm (4.0 inch) thick lead shield to

Table 1
Quartz cell specifications. The cell length and inner diameter were quoted (Starna, 2014) to have an uncertainty of 0.01 mm and 0.02 mm, respectively.

Cat. No.	Length	Inner diameter	Volume
35-Q-10	10 ± 0.01 mm	47 ± 0.02 mm	17 ml

Table 2
Isotopic analysis of uranium in the liquid samples by mass spectroscopy. The analysis was performed at ORNL.

Isotope	Atom %	Uncertainty
^{234}U	0.1182	0.0024
^{235}U	9.3498	0.1870
^{236}U	89.1480	0.8915
^{238}U	1.3827	0.0277

Table 3
Details for the thick liquid sample containing the highest concentration of ^{236}U from Reference (ORNL, 2013). The number density (second column) and the associated uncertainty (third column) shown for all isotopes (first column) were used in the analysis. The total number density for this sample is also included in the last row.

Thick liquid sample		
Highest concentration of ^{236}U		
Isotope	Number density (atoms/barn)	Uncertainty (atoms/barn)
^{234}U	2.4728×10^{-7}	4.9555×10^{-8}
^{235}U	1.9472×10^{-5}	3.1411×10^{-7}
^{236}U	1.8497×10^{-4}	2.9837×10^{-6}
^{238}U	2.8333×10^{-6}	6.7210×10^{-8}
H	3.0800×10^{-7}	4.3844×10^{-9}
D	6.2100×10^{-2}	8.8400×10^{-4}
N	1.3300×10^{-3}	1.8933×10^{-5}
O	3.4400×10^{-2}	4.8969×10^{-4}
Total	0.098	0.001

Table 4
Details for the medium liquid sample containing the medium concentration of ^{236}U from Reference (ORNL, 2013). The number density (second column) and the associated uncertainty (third column) shown for all isotopes (first column) were used in the analysis. The total number density for this sample is also included in the last row.

Medium liquid sample		
Medium concentration of ^{236}U		
Isotope	Number density (atoms/barn)	Uncertainty (atoms/barn)
^{234}U	1.6211×10^{-7}	3.2487×10^{-8}
^{235}U	1.2785×10^{-5}	2.0624×10^{-7}
^{236}U	1.2118×10^{-4}	1.9548×10^{-6}
^{238}U	1.8644×10^{-6}	4.4227×10^{-8}
H	3.0800×10^{-7}	4.3844×10^{-9}
D	6.2200×10^{-2}	8.8543×10^{-4}
N	1.3300×10^{-3}	1.8933×10^{-5}
O	3.4500×10^{-2}	4.9111×10^{-4}
Total	0.098	0.001

Table 5
Details for the thin liquid sample containing the lowest concentration of ^{236}U from Reference (ORNL, 2013). The number density (second column) and the associated uncertainty (third column) shown for all isotopes (first column) were used in the analysis. The total number density for this sample is also included in the last row.

Thin liquid sample		
Lowest concentration of ^{236}U		
Isotope	Number density (atoms/barn)	Uncertainty (atoms/barn)
^{234}U	1.0884×10^{-7}	2.1812×10^{-8}
^{235}U	8.5575×10^{-6}	1.3804×10^{-7}
^{236}U	8.1385×10^{-5}	1.3128×10^{-6}
^{238}U	1.2522×10^{-6}	2.9704×10^{-8}
H	3.1000×10^{-7}	4.4129×10^{-9}
D	6.2400×10^{-2}	8.8827×10^{-4}
N	1.3400×10^{-3}	1.9075×10^{-5}
O	3.4500×10^{-2}	4.9111×10^{-4}
Total	0.098	0.001

reduce ambient background counts.

All of the liquid samples were mounted on a computer controlled sample changer located approximately 12 m from the neutron production target. An empty quartz cell was also placed on the sample changer to measure the “open” beam count rate. A data run consisted of one complete cycle through all of the samples, with a predetermined number of LINAC bursts for each sample position. A series of 34 experimental runs of 50 min duration were performed, with time optimized for each sample to reduce statistical uncertainty in the resulting cross section.

The accelerator parameters for this experiment were an electron pulse rate of 225 pulses per second, an average current on target of 30 μA, and a beam energy of approximately 55 MeV.

A 0.159 cm (1/16 inch) thick cadmium filter was placed in the beam to minimize overlap of lower energy neutrons onto subsequent LINAC pulses. Also, a 3.493 cm (1.375 inch) thick lead filter was used throughout the experiment to attenuate gamma ray background emanating from the neutron production target (i.e., gamma flash).

A FastComTec P7889 multiscaler board was used to collect the TOF data into 51.2 ns time bins. The width of the stop pulse sent to the P7889 multiscaler was set equal to the 250 ns dead time of the detector system. During the experiment the dead time correction factor near the energy 5.467 eV was negligible ($\ll$1%).

Three moderated fission chambers located ≈9 m away from the production target were used to monitor the neutron beam intensity. Two of the fission chambers were Westinghouse WL6149A and the other was an Amperex B300D. These beam monitors were used to normalize the data to correct for any variations in the neutron beam intensity.

A gamma flash measurement was taken to establish the zero time for neutron time-of-flight and neutron burst width. The zero time was found to be 3.257 ± 0.007 μs (after correcting for the gamma ray flight time to the detector). The neutron burst width was found to be 240 ± 20 ns.

2.3. Background shape

Three fixed notches were included for all data runs, allowing for the determination of the time dependent background. A fixed notch is a material with a strong saturated resonance at an energy of interest and present for the entire measurement. The three fixed notches had saturated resonances at 1.5 eV (In), 18.6 eV (W), and 120 eV (Co). These three notch resonances were called “distant notches” since they are relatively far from the ^{236}U resonance at 5.467 eV. The distant notches were used to obtain the shape of the time dependent background. Additionally, a ^{238}U fixed notch was used which had a saturated resonance at 6.6 eV. This ^{238}U notch was called the “local notch” since it is close to the ^{236}U resonance at 5.467 eV ^{238}U was included in the experiment to be representative of the background magnitude at the ^{236}U resonance. The intended method was to use the In, W, and Co distant notches to fit the shape of the background and then normalize this shape to the ^{238}U local notch.

The distant notch data points for In, W, and Co were fitted with the RPI thermal transmission function (Danon, 1990) as seen in Fig. 1. This figure also shows the background shape normalized to the ^{238}U local notch at 6.6 eV. The background shape represents the contribution of both neutron and gamma rays. However, at this relatively low energy, the contribution from gamma rays (emanating from the neutron production target) is expected to be small. The background function is increasing with energy.

For all samples, the ^{238}U local notch data point was significantly higher than the other surrounding distant notches. A possible explanation is that the In, W, and Co distant notch resonances are

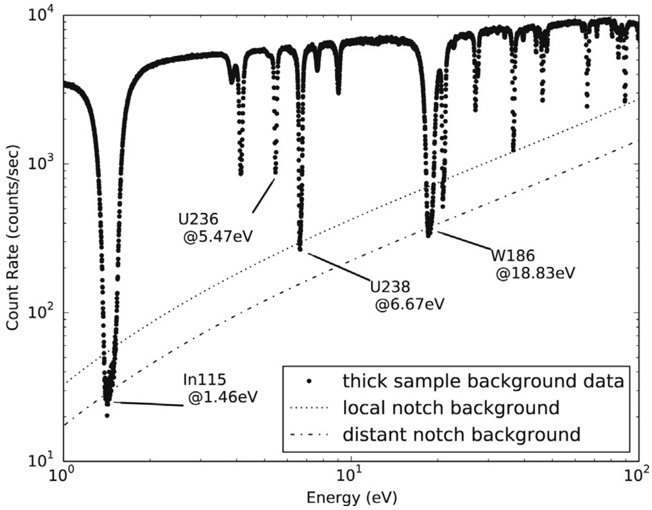

Fig. 1. Data used to determine the background for the resonance at 5.467 eV in the thick ^{236}U sample. Three fixed "distant" notches were placed in the neutron beam along with the thick ^{236}U sample. The distant notches with black resonances at 1.5 eV (In), 18.6 eV (W), and 120 eV (Co) were used to obtain the shape of the time dependent background. Additionally, a ^{238}U fixed "local" notch was placed in the neutron beam along with the thick ^{236}U sample and the "distant" notches. The local notch had a saturated resonance at 6.6 eV and was included to be representative of the background magnitude at the ^{236}U resonance. The local and distant backgrounds represent bounding values. Any background between the local and distant backgrounds was considered possible.

significantly more saturated (i.e., wider) than the ^{238}U local notch resonance.

The experiment was designed to balance two competing effects. If the fixed notch is too thick it will attenuate not only the beam, but also the background, creating a local depression in the background. Using these data would systematically lower the estimated background at the ^{236}U resonance. Conversely, if a fixed notch is too thin some small but significant fraction of the open beam is mixed with the background in the counts underneath the notch. No notch is ever fully saturated due to the exponential nature of the neutron attenuation with notch thickness. Since the signal is approximately 25 times larger than the background even a small fraction of open beam passing uncollided through the notch would introduce a systematic increase in the estimated background at the ^{236}U resonance. An optimized measurement would have a fixed notch with visible evidence that the resonance is saturated, i.e. a flat region at the bottom of the resonance, but not so saturated as to create a local depression in the background. The best fit (lowest χ^2) to the ^{236}U data occurred using a background close to midway between the local ^{238}U notch and the distant In and W notches. Therefore, the local and distant backgrounds represent bounding values. Any background between the local and distant backgrounds was considered possible. The difference between the distant notch background and the local notch background was considered the uncertainty in the overall background.

2.4. Transmission data

A TOF spectrum was collected for each ^{236}U liquid sample used in the transmission measurement. All of the TOF data were statistically checked to ensure that all samples experienced the same beam conditions. This statistical check was designed to identify LINAC malfunctions and any other problem that would lead to a loss of counts relative to the neutron beam monitors. Any data set that did not pass the integrity test was eliminated. The TOF data were then dead time corrected, normalized to beam monitors, and summed for each sample. Finally, the data were grouped into 409.6 ns width TOF bins to improve the point wise statistical uncertainties of the ^{236}U resonance at 5.467 eV.

The transmission in time-of-flight channel i is expressed as:

$$T_i = \frac{C_i^s - k_s B_i^s - B_s}{C_i^o - k_o B_i^o - B_o} \quad (2)$$

where T_i is the transmission, C_i^s and C_i^o are the sample and open beam count rates, B_i^s and B_i^o are the sample and open time-dependent backgrounds, k_s and k_o are normalization factors for the sample and open beam time dependent backgrounds, and B_s and B_o are the steady-state background counting rates for sample and open measurements.

As previously discussed in Section 2.3, there were two bounding background shapes. Each background shape led to a different transmission data set that was used in the Monte Carlo method explained in Section 2.6.

2.5. Resolution function

Equation (1) assumes ideal experimental conditions. The spectrometer system (LINAC, target, detector, etc.) has a finite resolving power such that the experimentally observed transmission, $T_{exp}(E)$, will be:

$$T_{exp}(E) = \int_{E1}^{E2} R_T(E - E')T(E')dE' \quad (3)$$

where $T(E')$ is the ideal transmission (Equation (1)) at energy E' and $R_T(E-E')$ is the experiment resolution function, normalized to have an area of unity. The resolution function represents the probability of detecting a neutron with energy E' at the same time as expected energy E. Equation (3) shows that the experimentally observed transmission is a convolution of the ideal transmission and the experimental resolution function. This convolution will result in a broadening of the measured transmission data and change the shape of the resonance.

The experimental transmission data were fitted with the R-matrix Bayesian statistics code SAMMY (Larson, 2008), which uses a shape analysis procedure to extract the resonance parameters. Since the effects of the resolution function may lead to changes in the shape of the resonance, it is crucial to know the resolution function and minimize its influence when possible. Inaccuracy in the resolution function would lead to incorrect resonance parameters.

The resolution function was found with SAMMY by fitting the RPI resolution function parameters (Appendix A) to the ^{238}U transmission data at 6.6 eV. This resonance has both the benefit of having repeated measurements in agreement which give confidence in the accuracy of the existing resonance parameters and is in close proximity to the ^{236}U resonance at 5.467 eV. This is advantageous since the resolution function varies slowly with energy. This resolution function fitting procedure has been used successfully and documented in prior work (Leinweber et al., 2010; Barry, 2003; Moretti, 1996; Danon, 1990).

The ^{238}U fixed notch, obtained in the open beam ^{236}U transmission experiment, was used as the ^{238}U sample-in data. This sample was natural uranium (99.27% ^{238}U) with a thickness of 0.5131 mm (0.0202 inches, 0.002336 a/b). The sample-out data was found by repeating the open beam ^{236}U transmission experiment without the ^{238}U fixed notch. The transmission (Equation (2)) was found for the 6.6 eV ^{238}U resonance by taking a ratio of the ^{238}U sample-in data to the ^{238}U sample-out data.

The background shape for the resolution function measurement was determined in the same manner as described in Section 2.3. Once again, the distant notches were used to obtain the background shape. With respect to the local notch background shape, the same sample-in and sample-out normalization values from Section 2.3 were used. It was assumed that the magnitude of the background in this resolution function measurement was also bounded by the distant background and local background shapes. This process resulted in two bounding resolution functions, one for each background shape, which are tabulated in Appendix A.

2.6. Monte Carlo method

For the past several years nuclear data scientists have been applying Monte Carlo methods to propagate uncertainties in nuclear data (Rochman et al., 2014; Smith, 2008). In particular, the work of Koning and Rochman (2008) used the Total Monte Carlo (TMC) method to propagate uncertainties in nuclear data to large scale nuclear reactor systems in order to obtain uncertainties on k_{eff} in criticality benchmarks. The TMC is a brute force method that performs the same simulation repeatedly while sampling all parameters of interest from probability distributions for each simulation.

The following SAMMY input values were randomly sampled within uncertainty from probability distributions: flight path (Gaussian), zero time (Gaussian), magnitude of each experimental data point (Gaussian), background normalization factors (uniform), temperature (Gaussian), sample thicknesses (Gaussian), burst width (Gaussian), resolution function parameters (uniform), energy range of fit (uniform), and order of the samples in the sequential calculation (uniform).

Although the TMC can be computationally expensive, this method was chosen since it is relatively easy to perform and incorporates non-linear effects.

The TMC method was used with the SAMMY code to find the RPI-2014 values and uncertainties on the ^{236}U resonance parameters at 5.467 eV (Table 6). This method repeats a SAMMY calculation N times, while randomly sampling input values to the code from probability distributions. Each probability distribution represents the level of uncertainty in the randomly sampled value. The process yields a solution vector of length N for each fitted parameter: E, Γ_γ, Γ_n, and normalization. The normalization was varied in the simulations to account for an offset in the baseline transmission in the potential scattering region. The final result for each fitted parameter is the arithmetic mean and standard deviation of each solution vector. The value of N was set equal to 1250 and was selected to ensure that the change in the standard deviation as a function of N converged to less than 0.2% for all solution vectors. The resonance parameter results of this method are presented in Table 6. The normalization was found to be 0.979 ± 0.004, reflecting a 2% correction in transmission which may be attributed to hydrogen introduced during sample manufacture. The fission width, Γ_f, was not fitted since it makes a negligible contribution to the RPI-2014 results but was included for completeness. In addition the RPI-2014 transmission measurement is not particularly sensitive to Γ_f since it only contributes ≈1% to the total cross section. The ENDF-7.1 value of Γ_f was used for the RPI-2014 results and reported with no uncertainty. Recent measurements by Sarmento et al. (2011) confirmed the value of Γ_f in JENDL-4.0 that is lower than ENDF-7.1 by an order of magnitude. However, utilizing the JENDL-4.0 value of Γ_f made no significant difference in our results.

The contribution to the overall uncertainty from each randomly sampled input value was investigated. The background, resolution function, and sample thickness were found to be the dominant contributors.

2.7. Neutron capture resonance integral

The ^{236}U resonance at 5.467 eV makes a large contribution to the thermal cross section point at 0.0253 eV. Therefore, the RPI-2014 resonance parameters for ^{236}U presented in this paper (Table 6) would imply a change in the thermal cross sections values relative to what is currently found in the nuclear data evaluations. However, the RPI-2014 transmission measurement data is not appropriate to recommend changes to the ^{236}U thermal values since the Cd filter removes a majority of the neutron flux below ≈0.5 eV. Therefore, the thermal values used in ENDF-7.1 were preserved to within 0.5% by fitting the negative resonance parameters with SAMMY, while keeping the RPI-2014 ^{236}U resonance parameters at 5.467 eV (Table 6) constant. All parameters from higher energy resonances were taken from ENDF-7.1. The resulting negative energy level parameters are found in Table 7.

Table 7
The RPI-2014 negative resonance parameter values for ^{236}U were fitted with SAMMY while keeping the resonance parameters for the 5.467 eV resonance fixed to the RPI-2014 resonance values given in Table 6. All resonance parameters from higher energy were taken from ENDF-7.1. This method preserved the thermal cross section values of ENDF-7.1 to within 0.5%.

E (eV)	Γ_γ (meV)	Γ_n (meV)	Γ_f (meV)
−9.7	21.4	4.909	0.08

Table 6
Summary of the ^{236}U resonance parameters at 5.467 eV and the resulting peak total neutron cross sections. The RPI-2014 resonance parameters were calculated with the Total Monte Carlo method described in Section 2.6. The RPI-2014 fission width, Γ_f, was fixed at the ENDF-7.1 value without any uncertainty. The NJOY code (MacFarLane and Muir, 1994) was used to calculate the peak cross section of ^{236}U at 5.467 eV, Doppler broadened to 300 K. When calculating the peak cross section for Harvey and Hughes, the Carlson et al. value for Γ_γ was used.

Reference	E (eV)	Γ_γ (meV)	Γ_n (meV)	Γ_f (meV)	σ_T^{peak} (barns)
RPI-2014 (current work)	5.467 ± 0.005	27 ± 1	2.13 ± 0.04	0.290	13571
Mughabghab (2006)	5.45 ± 0.03	24.7 ± 0.6	2.19 ± 0.08	0.290 ± 0.073	14316
ENDF-7.1 (Chadwick et al., 2011)	5.45	24.5	2.24	0.290	14665
JEFF-3.2 (Koning et al., 2006)	5.45	24.5	2.16	0.290	14152
JENDL-4.0 (Shibata et al., 2011)	5.456	24.5	2.30	0.018	15070
Carlson et al. (1970)	5.45 ± 0.03	24.5 ± 1	2.16 ± 0.08	Not reported	14192
Baumann et al. (1968)	5.48	32.5 ± 3.5	2.4 ± 0.25	Not reported	14478
McCallum (1958)	5.48 ± 0.06	29 ± 7	1.95 ± 0.4	Not reported	12207
Harvey and Hughes (1958)	5.49 ± 0.049	Not reported	1.76 ± 0.21	Not reported	11495

The infinitely dilute neutron capture resonance integral (RI_γ) was calculated as follows:

$$RI_\gamma = \int_{0.5\ \text{eV}}^{20\ \text{MeV}} \sigma_\gamma(E)\frac{dE}{E} \quad (4)$$

where $\sigma_\gamma(E)$ is the neutron capture cross section in barns, Doppler broadened to a temperature of 300 K, at energy E in eV. The RPI-2014 calculation used the ENDF-7.1 resonance parameters for ^{236}U, substituting the RPI-2014 values shown in Table 6 for the 5.467 eV resonance and the values in Table 7 for the negative energy resonance. The results for RPI-2014 and several evaluation libraries are shown in Table 8. The neutron capture resonance integral was calculated using a combination of the NJOY (MacFarLane and Muir, 1994) and INTER (Dunford, 2001) codes. The uncertainty on the resonance integral was found by application of the TMC method. The NJOY and INTER calculations were performed repeatedly while randomly sampling each of the RPI-2014 ^{236}U resonance parameters from a Gaussian distribution. The width of each Gaussian distribution was defined as the uncertainty on the resonance parameter of interest. The reported uncertainty on the capture resonance integral is the standard deviation of the results. The calculations were repeated 2000 times to ensure that the standard deviation of the capture resonance integral converged to less than 0.1%.

3. Results and discussion

The methods described in this paper yielded the parameters of the ^{236}U resonance at 5.467 eV. The values of the RPI-2014 resonance parameters are shown in the first row of Table 6. The use of liquid samples allowed for non-saturated resonances. The quality of the RPI-2014 resonance parameters is demonstrated by their ability to accurately fit the shape of the neutron transmission resonance data for all three samples as shown in Fig. 2.

Table 6 also includes the nuclear data evaluations of Mughabghab (2006), ENDF-7.1 (Chadwick et al., 2011), JEFF-3.2 (Koning et al., 2006), and JENDL-4.0 (Shibata et al., 2011) along with the previous experimental results of Carlson et al. (1970), Baumann et al. (1968), Harvey and Hughes (1958), and McCallum (1958). The RPI-2014 value of Γ_n for the 5.467 eV resonance in ^{236}U is lower than all values presently found in the selected nuclear data evaluations. The RPI-2014 value of Γ_n is lower than Mughabghab by 2.8%, lower than ENDF-7.1 by 5.2%, lower than JEFF-3.2 by 1.4%, and lower than JENDL-4.0 by 8.0%. However, the current RPI-2014 value of Γ_n agrees with Mughabghab and JEFF-3.2 to within uncertainties. When compared to previous experimental results, the RPI-2014 value of Γ_n is lower than Carlson et al. by 1.4%, lower than Baumann et al. by 12.7%, greater than Harvey and Hughes by 21%, and greater than

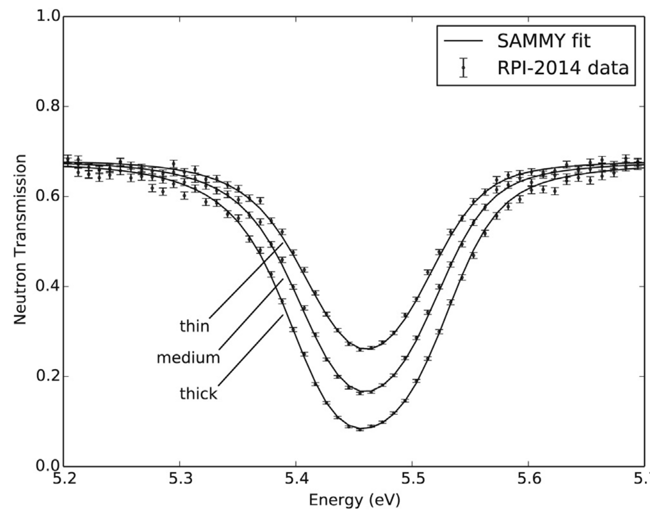

Fig. 2. RPI-2014 data from the ^{236}U transmission measurement at 5.467 eV. The symbols are the error bars for the RPI-2014 data points determined from the counting statistics from the measurement. Three enriched ^{236}U liquid samples were used and designated as thin, medium, and thick (Section 2.1). The solid lines for all samples were calculated from the RPI-2014 resonance parameters, which were found with the Total Monte Carlo method (Section 2.6) using the SAMMY code. The ability of the RPI-2014 parameters to accurately fit the shape of all three samples shows the quality of the results.

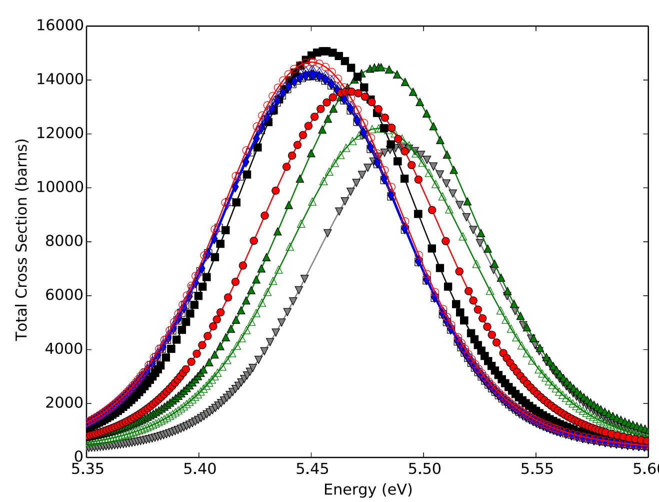

Fig. 3. The total cross section for the 5.467 eV resonance in ^{236}U using the parameters for each reference in Table 6 is shown. The NJOY code was used to construct and Doppler broaden (300 K) each plot. The peak total cross section for RPI-2014 (●) is lower than Mughabghab (◊), ENDF-7.1 (○), JEFF-3.2 (□), JENDL-4.0 (■), Carlson et al. (♦), and Baumann et al. (▲). Conversely, the peak total cross section for RPI-2014 is greater than McCallum (△) and Harvey et al. (▼). The energy of the RPI-2014 total cross section resonance at 5.467 eV is noticeably different when compared the other total cross section data but is within previously reported uncertainties. The solid lines are meant to serve as eye guides between the data points. The total cross section of Mughabghab, Carlson et al., and JEFF-3.2 are indistinguishable since their resonance parameters are almost identical.

Table 8
Comparison of the ^{236}U neutron capture resonance integral (RI_γ) for RPI-2014 and selected nuclear data evaluations. The RPI-2014 value was calculated using ENDF-7.1 resonance parameters for ^{236}U, while substituting the RPI-2014 values shown in Table 6 for the 5.467 eV resonance and the values in Table 7 for the negative energy resonance. The neutron capture resonance integral was calculated using a combination of the NJOY (MacFarLane and Muir, 1994) and INTER (Dunford, 2001) codes. The value for Mughabghab was taken from the Atlas of Neutron Resonances (Mughabghab, 2006).

Data source	RI_γ (barns)
RPI-2014	330 ± 5
Mughabghab	345 ± 15
ENDF-7.1	342
JEFF-3.2	346
JENDL-4.0	353

McCallum by 9.2%. With the exception of Harvey and Hughes, the RPI-2014 result for Γ_n agrees with the previous experimental data within uncertainties.

Table 6 shows that the RPI-2014 value of Γ_γ for the 5.467 eV resonance in ^{236}U is higher than the nuclear data evaluations and Carlson et al. The RPI-2014 value of Γ_γ is greater than Mughabghab by 9.3% and greater than ENDF-7.1, JEFF-3.2, JENDL-4.0 and Carlson et al. by 10.2%. The RPI-2014 value of Γ_γ is less than the previous experimental results of Baumann et al. by 20.4% and less than McCallum by 7.4%. The RPI-2014 result for Γ_γ is within the quoted uncertainty of McCallum.

The RPI-2014 value of 5.467 eV for the ^{236}U resonance energy in Table 6 is higher than all of the selected nuclear data evaluations and Carlson et al. by about 0.3% and less than the remaining experimental results by about 0.2–0.4%. The RPI-2014 result for the energy value is within previously reported uncertainties.

The ^{236}U resonance parameters at 5.467 eV were used to construct the total cross section (Fig. 3) using the NJOY code. The cross section was Doppler broadened to a temperature of 300 K and the peak value was obtained. The total cross section of plots of Mughabghab, Carlson et al., and JEFF-3.2 are indistinguishable since their resonance parameters are almost identical. The peak total cross section values are included in the last column of Table 6. The Carlson et al. value for Γ_γ was used in the case of Harvey and Hughes.

Table 7 shows the negative energy resonance parameters in ^{236}U that were fitted with the SAMMY code in order to preserve the thermal cross section values to within 0.5% of ENDF-7.1. The RPI-2014 negative energy parameters are very close to the original ENDF-7.1 parameters.

The NJOY and INTER codes were used to calculate the ^{236}U capture resonance integral using the RPI-2014 parameters for the negative energy (Table 7) and the 5.467 eV resonance (Table 6). The resulting RPI-2014 capture resonance integral is compared to the selected nuclear data libraries in Table 8. The results show that the RPI-2014 capture resonance integral is lower than all of the selected nuclear data evaluations: Mughabghab by 4.7%, ENDF-7.1 by 3.7%, JEFF-3.1 by 4.8% and JENDL-4.0 by 7.2%.

4. Conclusions

High accuracy transmission measurements were performed at the RPI LINAC to determine the resonance parameters of the ^{236}U resonance at 5.467 eV. The resonance parameters determined in this work show a decrease in the peak total cross section for the ^{236}U resonance at 5.467 eV when compared with the current evaluations of Mughabghab, ENDF-7.1, JEFF-3.2, and JENDL-4.0. These parameters result in a lower neutron capture resonance integral with respect to the current evaluations.

Appendix A. Resolution function

The SAMMY code allows the user to choose from several different predefined resolution functions. This paper utilized the RPI resolution function, which represents the combined effects of the neutron producing target moderator and the detector system using a chi-squared function plus two exponential terms. The mathematical form of the RPI resolution function is explicitly defined in the SAMMY manual (Larson, 2008). The fitted RPI resolution function parameters used in this paper are shown in Table (A.1) for the local and distant background shapes as discussed in Section 2.5.

Table A.1
The RPI Resolution Function parameters used in SAMMY (Larson, 2008). The local (column 2) and distant (column 3) parameters represent the resolution function when using the local and distant background shapes explained in Section 2.3.

Parameter	Local	Distant	units
τ_1	234.67178	277.50783	ns
τ_2	2.5346E-02	2.5925E-02	1/eV
τ_3	237.72025	280.84240	ns
τ_4	3.0740E-02	3.1504E-02	1/eV
τ_5	176.81659	196.48548	ns
Λ_0	529.04249	391.45612	ns
Λ_1	−215.32856	−162.51178	ns
Λ_2	21.89386	24.09497	ns
a_1	−4.2708E-04	−2.6777E-04	1/ns
a_2	2.4076E-02	2.4076E-02	1/eV
a_3	−6.3000E-04	−6.3000E-04	1/ns
a_4	3.53100	3.53100	1/eV
a_5	1.5368E-03	1.7303E-03	1/ns
t_0	931.88413	929.11081	ns
A_2	−70.52550	−71.89694	none
A_3	4.9918E-03	4.9825E-03	1/ns
A_4	0.39671	0.39818	none
A_5	7.2725E-04	6.4313E-04	1/ns

References

Barry, D., 2003. Neodymium Neutron Transmission and Capture Measurements and the Design of an Improved Resolution Transmission Detector. Ph.D. thesis. Rensselaer Polytechnic Institute.

Baum, E., Ernesti, M., Knox, H., Miller, T., Watson, A., 2010. Nuclide and Isotopes Chart of the Nuclides, seventeenth ed. Bechtel Marine Propulsion Corporation.

Baumann, P., Halford, J., Pellarin, D., 1968. Resonance parameters for ^{236}U from integral measurements. Nucl. Sci. Eng. 32, 265.

Carlson, A., Friesenhahn, S., Lopez, W., Fricke, M., 1970. The ^{236}U neutron capture cross section. J. Nucl. Phys. A 141, 577.

Chadwick, M., Herman, M., Oblozinsky, P., et al., 2011. ENDF/B-VII.1 nuclear data for science and technology: cross sections, covariances, fission product yields and decay data. Nucl. Data Sheets 112, 2887–2996.

CINDA, 2014. Computer Index of Nuclear Reaction Data (CINDA), Database Version June 2014. Information extracted from online CINDA database. www-nds.iaea.org/exfor/cinda.htm.

Danon, Y., 1990. Design and Construction of the RPI Enhanced Thermal Target and Thermal Cross Section Measurements of Rare Earth Isotopes. Ph.D. thesis. Rensselaer Polytechnic Institute.

Dunford, C., 2001. ENDF Utility Codes Release 6.12 (Informal Report).

Harvey, J., Hughes, D., 1958. Spacings of nuclear energy levels. Phys. Rev. 109, 471.

Koning, A., Forrest, R., Kellett, M., et al., 2006. The JEFF-3.1 Nuclear Data Library. Nuclear Energy Agency.

Koning, A., Rochman, D., 2008. Towards sustainable nuclear energy: putting nuclear physics to work. Ann. Nucl. Energy 35, 2024–2030.

Larson, N., 2008. Updated Users' Guide for SAMMY: Multilevel R-matrix Fits to Neutron Data Using Bayes' Equations. ORNL/TM-9179/R8. Oak Ridge National Laboratory.

Leinweber, G., Barry, D., Burke, J., Drindak, N., Block, R., Danon, Y., Moretti, B., 2010. Resonance parameters and their uncertainties derived from epithermal neutron capture and transmission measurements of elemental molybdenum. Nucl. Sci. Eng. 164, 287–303.

MacFarLane, R., Muir, D., 1994. The NJOY Nuclear Data Processing System Version 91. LA-12740-M. Los Alamos National Laboratory.

McCallum, G., 1958. The neutron total cross-sections of uranium-234 and uranium-236. J. Nucl. Eng. 6, 181.

Moretti, B., 1996. Molybdenum Neutron Transmission Measurements and the Development of an Enhanced Resolution Neutron Target. Ph.D. thesis. Rensselaer Polytechnic Institute.

Mughabghab, S., 1984. Neutron Cross Sections, vol. 1B. Academic Press, Orlando, Florida.

Mughabghab, S., 2006. Atlas of Neutron Resonances, fifth ed. Elsevier, New York.

ORNL, 2013. Oak Ridge National Laboratory, Isotope Business Office, Work authorization 65-0218-1.

Rochman, D., Zwermann, W., van der Marck, S., Koning, A., Sjöstrand, H., Helgesson, P., Krzykacz-Hausmann, B., 2014. Efficient use of Monte Carlo: uncertainty propagation. Nucl. Sci. Eng. 177, 337–349.

Sarmento, R., Calviani, M., Praena, J., et al., 2011. Measurement of the ^{236}U(n,f) Cross Section from 170 meV to 2 MeV at the CERN n_TOF Facility. Phys. Rev. C 84, 044618.

Shibata, K., Iwamoto, O., Nakagawa, T., et al., 2011. JENDL 4.0: a new library for nuclear science and engineering. J. Nucl. Sci. Technol. 48, 1–30.

Smith, D., 2008. A Unified Monte Carlo Approach to Fast Neutron Cross Section Data Evaluation. ANL/NDM-166. Argonne National Laboratory.

Starna, 2014. Starna Cells. Inc., PO Box 1919, Atascadero, CA 93423 USA. www.starnacells.com.